Information Exchange in Multi-rover SLAM

Brandon M. Jones and Lang Tong
School of Electrical and Computer Engineering
Cornell University, Ithaca, NY 14853
{bmj34,lt35}@cornell.edu

Abstract – *We investigate simultaneous localization and mapping (SLAM) involving multiple robots through collaborations. In particular, we assume that robots may communicate to each other when in communication range. Several scenarios are considered: (i) robots fully able to communicate while conducting SLAM; (ii) robot communications are intermittent due to each robot having a limited but equal communication range; (iii) communications among robots are asymmetrical in that some robots may have a larger communication range than other robots. In this paper, we develop a model for multi-robot SLAM and include mechanisms for information exchange. We also provide performance comparisons for various cases of multi-robot and single-robot SLAM based on algorithms we develop to incorporate exchanged information.*

Keywords: Space robotics, multi-robot systems, Kalman filtering, simultaneous localization and mapping (SLAM).

1 Introduction

Future missions to the moon, and longer-term missions to Mars, may require the use of multiple rovers to complete practical tasks such as autonomous terrain exploration and transportation of regolith and products of in-situ resource utilization (ISRU) plants between various locations or facilities at a lunar outpost. To effectively complete such tasks, future rovers will require the ability to operate in both structured and unstructured environments, as independent platforms and as coordinated robotic formations to assist astronauts in lunar operations. In particular, the capability of the rovers to conduct simultaneous localization and mapping (SLAM) both independently and as teams may contribute to overall mission success.

In this paper, we focus on the benefits of communication using a formation model for multi-rover SLAM. Part of this is not new; for instance, it has been shown that (over short distances, yet in the presence of intermittent satellite communication) using trilateration in conjunction with various robot formations can contribute to the reduction of estimation error within a rover formation [1]. Although this localization approach is based on the extended Kalman filter (EKF) [2], it does not simultaneously estimate stationary landmarks as necessary for EKF-based SLAM algorithms. In addition, another component of this approach is the use of block diagonal system matrices to model inherently coupled formations (and as far as we know, block diagonal system matrices are also used for every other current state-space based approach to the multi-robot SLAM problem). The basic intuition behind the use of block diagonals is to implement coordinate transformations between the robots [3], yet such an approach does not model the coupling (if any) within the robot team. Also, and more generally, information between mobile robot platforms can be coordinated through the use of the channel filter [4] (however, in regards to exchanging formation information, channel filters do not communicate vehicle data [5]) and the sparse extended information filter (SEIF) [6], which is a particle filter based approach mainly used for global localization problems. Decision theoretic strategies have also been considered [7]. The main idea of our approach is to introduce coupling of the rover states by relaxing the assumption of a block diagonal system matrix and to demonstrate a leader-follower formation that explicitly models coupling between rover states while implementing SLAM.

The core of this paper is the next section on linear formation models for multi-robot SLAM. Sections 2.1-2.2 provide the linear models associated with SLAM based on Kalman filtering; basic illustrations are also provided to demonstrate the physical impact of noise within each model. Section 2.3 presents a leader-follower model which we later use to show the performance of SLAM with multiple robots when the robot states are coupled (mainly due to a system matrix that models coupling between rovers). The state estimator based on the leader-follower model is given in Section 2.4. Results and example applications are provided in Section 2.5.

2 Models

In this section, we present the linear kinematic and measurement models associated with SLAM based on Kalman filters, which are used as baselines to construct equivalent state and measurement spaces for a leader-follower model. The more general case for EKF-based SLAM [8] based on a nonlinear leader-follower model is considered as future work.

2.1 Single-robot kinematic model

The state of a single rover i at time k is denoted as $\mathbf{x}^i_{v,k} = [x^i_k \;\; y^i_k \;\; \phi^i_k]^\top$ (the subscript v is the traditional notation for a vehicle state). The state vector of a stationary landmark n is $\mathbf{x}_{L_n} = [x_{L_n} \;\; y_{L_n}]^\top$. The SLAM system model for rover i with N landmarks is then

$$\begin{bmatrix} \mathbf{x}^i_{v,k} \\ \mathbf{x}_{L_1} \\ \vdots \\ \mathbf{x}_{L_N} \end{bmatrix} = \begin{bmatrix} \mathbf{A}^i_{v,k} & & & \\ & \mathbf{I} & & \\ & & \ddots & \\ & & & \mathbf{I} \end{bmatrix} \begin{bmatrix} \mathbf{x}^i_{v,k-1} \\ \mathbf{x}_{L_1} \\ \vdots \\ \mathbf{x}_{L_N} \end{bmatrix} + \begin{bmatrix} \mathbf{u}^i_{v,k} \\ \mathbf{0} \\ \vdots \\ \mathbf{0} \end{bmatrix} + \begin{bmatrix} \mathbf{w}^i_{v,k} \\ \mathbf{0} \\ \vdots \\ \mathbf{0} \end{bmatrix} \tag{1}$$

$$\mathbf{x}^i_k = \mathbf{A}^i_k \mathbf{x}^i_{k-1} + \mathbf{u}^i_k + \mathbf{w}^i_k \tag{2}$$

which includes the control vector $\mathbf{u}^i_{v,k}$ and system matrix $\mathbf{A}^i_{v,k}$ of the rover. The noise associated with the kinematics of rover i is modeled by the Gaussian random variable $\mathbf{w}^i_{v,k} \sim \mathcal{N}(\mathbf{0}, \mathbf{Q}^i_{v,k})$. The matrix $\mathbf{Q}^i_{v,k} = \sigma^2_w \mathbf{I}$ is known as the kinematic noise covariance matrix, where σ_w is the standard deviation of the kinematic noise term. The physical impact of noise within the system model is shown in Figure 1.

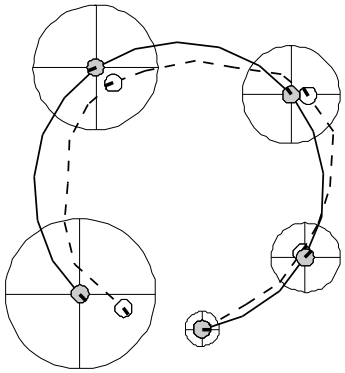

Figure 1: Illustration of kinematic noise. A nominal rover trajectory (solid line) is subject to kinematic noise, often resulting in random trajectory deviations (dashed line). The impact of kinematic noise may be "small" over tiny intervals, but often it accumulates over time.

2.2 Single-robot measurement model

A measurement of landmark n at time k by rover i is denoted as $\mathbf{y}^i_{k,L_n}$; note, however, that 1) the vector $\mathbf{y}^i_{k,L_n}$ is a *single* landmark measurement and that 2) the number of landmark measurements at any particular time-step k depends on both the pose of the rover $\mathbf{x}^i_{v,k}$ and the surrounding environment. For instance, a measurement of landmark 1 by rover i at time k is simply given by the vector $\mathbf{y}^i_{k,L_1}$, but a measurement of, say, landmarks 1 and 3 is given by the vector $[(\mathbf{y}^i_{k,L_1})^\top \;\; (\mathbf{y}^i_{k,L_3})^\top]^\top$. The measurement matrix of $\mathbf{y}^i_{k,L_n}$ is $\mathbf{C}^i_k = [\,\mathbf{C}^i_{v,k} \;\; \mathbf{C}^i_{k,L_n}]$, where the matrix $\mathbf{C}^i_{k,L_n}$ "selects" landmark n from the N-landmark vector. It follows that the measurement of landmark n by rover i is modeled as

$$\mathbf{y}^i_{k,L_n} = \begin{bmatrix} \mathbf{C}^i_{v,k} & \mathbf{C}^i_{k,L_n} \end{bmatrix} \begin{bmatrix} \mathbf{x}^i_{v,k} \\ \mathbf{x}_{L_1} \\ \vdots \\ \mathbf{x}_{L_N} \end{bmatrix} + \mathbf{v}^i_{k,L_n} \tag{3}$$

$$= \mathbf{x}_{L_n} + \mathbf{C}^i_{v,k} \mathbf{x}^i_{v,k} + \mathbf{v}^i_{k,L_n}. \tag{4}$$

The noise associated with this measurement is modeled by the Gaussian random variable $\mathbf{v}^i_{k,L_n} \sim \mathcal{N}(\mathbf{0}, \mathbf{R}^i_{k,L_n})$. The matrix $\mathbf{R}^i_{k,L_n} = \sigma^2_v \mathbf{I}$ is known as the measurement noise covariance matrix, where σ_v is the standard deviation of the measurement noise term (in this case, the subscript v is in the context of measurement noise). The impact of noise within the measurement model is illustrated below in Figure 2.

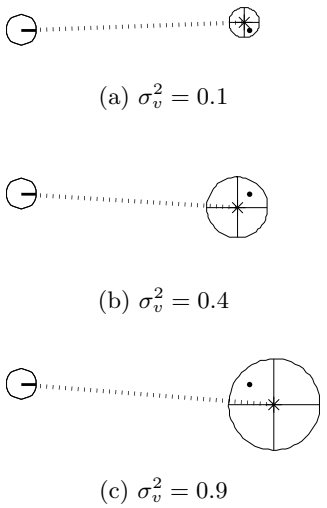

(a) $\sigma^2_v = 0.1$

(b) $\sigma^2_v = 0.4$

(c) $\sigma^2_v = 0.9$

Figure 2: Illustration of measurement noise. Although landmarks (black dots) are assumed to be stationary, the accuracy of landmark measurements (cross hairs) varies as a function of the sensor variance σ^2_v. The line-of-sight for each measurement is shown by vertical bars.

2.3 Leader-follower model

This sections applies Sections 2.1-2.2 to develop a leader-follower based formation model. The formations that result from implementing the models of this section most closely resemble formations of the column type [9] with a directed communication topology [10] at each time-step between the leader and follower rovers.

2.3.1 Leader process

We assume the *leader* rover, with assignment $i = 1$ and state $\mathbf{x}^1_{v,k}$ at time k, moves independently of any rover *followers* within a rover formation. The leader kinematic model is given by

$$\mathbf{x}^1_{v,k} = \mathbf{A}^1_{v,k}\mathbf{x}^1_{v,k-1} + \mathbf{u}^1_{v,k} + \mathbf{w}^1_{v,k}. \tag{5}$$

2.3.2 Follower process and control

We consider the case of a single *follower* rover, with assignment $i = 2$ and state $\mathbf{x}^2_{v,k}$ at time k. The leader control vector $\mathbf{u}^1_{v,k}$ may be computed by the robot (autonomous operation) or user-defined via tele-operational commanding from an outpost. However, we define the follower kinematics and control policy as

$$\mathbf{x}^2_{v,k} = \mathbf{x}^2_{v,k-1} + \mathbf{u}^2_{v,k} + \mathbf{w}^2_{v,k} \tag{6}$$

$$\mathbf{u}^2_{v,k} = \mu\left(\mathbf{x}^1_{v,k-1} - \mathbf{x}^2_{v,k-1}\right) + \widetilde{\mathbf{u}}^2_{v,k} \tag{7}$$

respectively, where μ such that $0 \leq \mu < 1$ determines the magnitude of the follower control and $\widetilde{\mathbf{u}}^2_{v,k}$ is the local control vector based on decisions of the follower.

2.3.3 Leader-follower kinematics

It follows from the definitions of the leader and follower dynamics in Equations 5-6, respectively, that we may extend Equation 1 as

$$\begin{bmatrix} \mathbf{x}^1_{v,k} \\ \mathbf{x}^2_{v,k} \\ \mathbf{x}_{L_1} \\ \vdots \\ \mathbf{x}_{L_N} \end{bmatrix} = \begin{bmatrix} \mathbf{I} & \mathbf{0} & & & \\ \mu\mathbf{I} & \mathbf{I}-\mu\mathbf{I} & & & \\ & & \mathbf{I} & & \\ & & & \ddots & \\ & & & & \mathbf{I} \end{bmatrix} \begin{bmatrix} \mathbf{x}^1_{v,k-1} \\ \mathbf{x}^2_{v,k-1} \\ \mathbf{x}_{L_1} \\ \vdots \\ \mathbf{x}_{L_N} \end{bmatrix} + \begin{bmatrix} \mathbf{u}^1_{v,k} \\ \widetilde{\mathbf{u}}^2_{v,k} \\ \mathbf{0} \\ \vdots \\ \mathbf{0} \end{bmatrix} + \begin{bmatrix} \mathbf{w}^1_{v,k} \\ \mathbf{w}^2_{v,k} \\ \mathbf{0} \\ \vdots \\ \mathbf{0} \end{bmatrix} \tag{8}$$

$$\mathbf{x}_k = \mathbf{A}_k\mathbf{x}_{k-1} + \mathbf{u}_k + \mathbf{w}_k. \tag{9}$$

The physical impact of Equation 9 is that the dynamics of $\mathbf{x}^1_{v,k}$ and $\mathbf{x}^2_{v,k}$ are coupled by the structure of the system formation matrix $\mathbf{A}_k$.

2.3.4 Measurement model

For measurements $\mathbf{y}^1_{k,L_n}$ of landmark n by rover $i = 1$ (the leader rover) and $\mathbf{y}^2_{k,L_m}$ of landmark m by rover $i = 2$ (the follower rover), the measurement model of Equation 3 can be extended to Equation 8 as

$$\begin{bmatrix} \mathbf{y}^1_{k,L_n} \\ \mathbf{y}^2_{k,L_m} \end{bmatrix} = \begin{bmatrix} \mathbf{C}^1_{v,k} & \mathbf{0} & \mathbf{C}^1_{k,L_n} \\ \mathbf{0} & \mathbf{C}^2_{v,k} & \mathbf{C}^2_{k,L_m} \end{bmatrix} \begin{bmatrix} \mathbf{x}^1_{v,k} \\ \mathbf{x}^2_{v,k} \\ \mathbf{x}_{L_1} \\ \vdots \\ \mathbf{x}_{L_N} \end{bmatrix} + \begin{bmatrix} \mathbf{v}^1_{k,L_n} \\ \mathbf{v}^2_{k,L_m} \end{bmatrix}$$

$$= \begin{bmatrix} \mathbf{x}_{L_n} + \mathbf{C}^1_{v,k}\mathbf{x}^1_{v,k} \\ \mathbf{x}_{L_m} + \mathbf{C}^2_{v,k}\mathbf{x}^2_{v,k} \end{bmatrix} + \begin{bmatrix} \mathbf{v}^1_{k,L_n} \\ \mathbf{v}^2_{k,L_m} \end{bmatrix} \tag{10}$$

for $n, m \in \{1, \ldots, N\}$. Similar to the single robot measurement model (Section 2.2), the number of landmark measurements will change depending on the pose of each rover (and subsequently, the configuration of the formation) within the environment for each time instance k.

2.4 Estimation model

Using the kinematic and measurement models of Section 2.3, we can now pose the leader-follower model in the context of Kalman filter based SLAM [11]. The prediction-step, or *time-update*, is computed as

$$\hat{\mathbf{x}}_{k|k-1} = \mathbf{A}_k\hat{\mathbf{x}}_{k-1|k-1} + \mathbf{B}_k\mathbf{u}_k \tag{11}$$

$$\mathbf{P}_{k|k-1} = \mathbf{A}_k\mathbf{P}_{k-1|k-1}\mathbf{A}_k^\top + \mathbf{Q}_k \tag{12}$$

meaning the estimate of $\mathbf{x}_k$ before incorporating measurements is distributed as a multivariate Gaussian $\mathcal{N}(\hat{\mathbf{x}}_{k|k-1}, \mathbf{P}_{k|k-1})$. For the correction-step, or *measurement update*, the innovation matrix $\mathbf{S}_k$ and Kalman gain $\mathbf{W}_k$ is computed as

$$\mathbf{S}_k = \mathbf{C}_k\mathbf{P}_{k|k-1}\mathbf{C}_k^\top + \mathbf{R}_k \tag{13}$$

$$\mathbf{W}_k = \mathbf{P}_{k|k-1}\mathbf{C}_k^\top\mathbf{S}_k^{-1} \tag{14}$$

followed by incorporating $\mathbf{y}_k$, the measurement vector at time k (assuming measurements are available), and the expected measurement vector $\hat{\mathbf{y}}_k$ as

$$\hat{\mathbf{x}}_{k|k} = \hat{\mathbf{x}}_{k|k-1} + \mathbf{W}_k\left(\mathbf{y}_k - \hat{\mathbf{y}}_k\right) \tag{15}$$

$$\mathbf{P}_{k|k} = \mathbf{P}_{k|k-1} - \mathbf{W}_k\mathbf{S}_k\mathbf{W}_k^\top \tag{16}$$

meaning the estimate of $\mathbf{x}_k$ after incorporating measurements is distributed as $\mathcal{N}(\hat{\mathbf{x}}_{k|k}, \mathbf{P}_{k|k})$.

2.5 Communication model

We use a simple disk model [12] to model whether or not two mobile rovers are within a certain communication range r. When the rovers are out of communication range, the rovers operate independently (Sections 2.1-2.2) and do not exchange information. However, if the leader state $\mathbf{x}^1_{v,k}$ and follower state $\mathbf{x}^2_{v,k}$ is such that

$$||\mathbf{x}^1_{v,k} - \mathbf{x}^2_{v,k}|| \leq r \tag{17}$$

then the communication may be 1) symmetric in that the communication range of both rovers equals r or 2) asymmetric if the communication range of one rover equals r while the other rover has a significantly larger communication range.

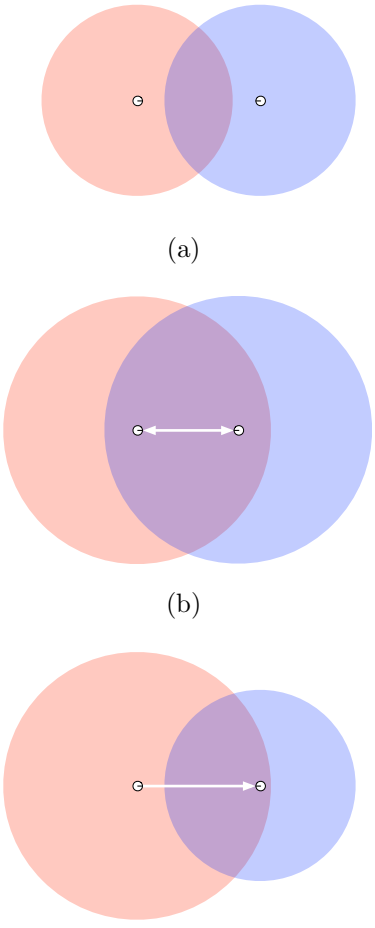

(a)

(b)

(c)

Figure 3: Topologies when two mobile rovers are (a) out of communication range, (b) exchanging information within an equal communication range and (c) both transmitting information with receptions received by only one of the rovers.

3 Results

This section provides basic examples of the leader-follower model and performance results of multi-robot SLAM with exchange of leader-follower information. An example of multi-robot SLAM for space applications is also provided for rovers operating at the location of a lunar outpost.

3.1 Leader-follower implementations

In Section 2.3, we defined a kinematic model with system matrix $\mathbf{A}_k$ that models the coupling between a leader state $\mathbf{x}^1_{v,k}$ and follower state $\mathbf{x}^2_{v,k}$ for a formation of two mobile rovers capable of implementing SLAM. Example trajectories resulting from this model are shown below in Figures 4-5. Figure 6 illustrates trajectories based on a multi-robot SLAM example that contains a "blind" follower (a rover incapable of collecting landmark measurements).

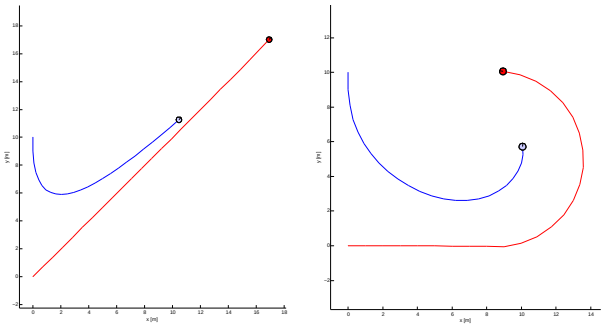

Figure 4: Nominal rover trajectories based on the leader-follower model (Section 2.3.3).

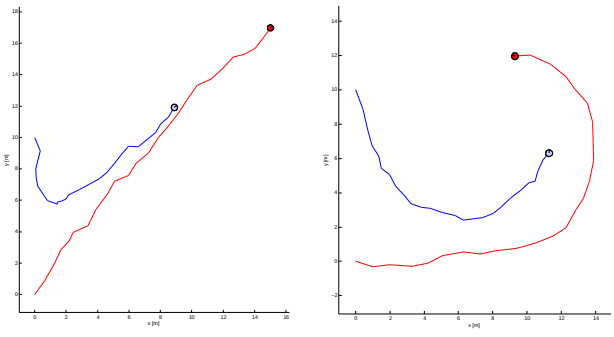

Figure 5: Trajectory realizations subjected to zero-mean and Gaussian kinematic noise.

One may notice from Figures 5-6 that the follower control policy will consist of imperfect state information, namely $\hat{\mathbf{x}}^i_{v,k-1|k-1}$ for each rover i and time k. In the context of Section 2.4, the follower control policy is then

$$\mathbf{u}^2_{v,k} = \mu\left(\hat{\mathbf{x}}^1_{v,k-1|k-1} - \hat{\mathbf{x}}^2_{v,k-1|k-1}\right) + \widetilde{\mathbf{u}}^2_{v,k}. \tag{18}$$

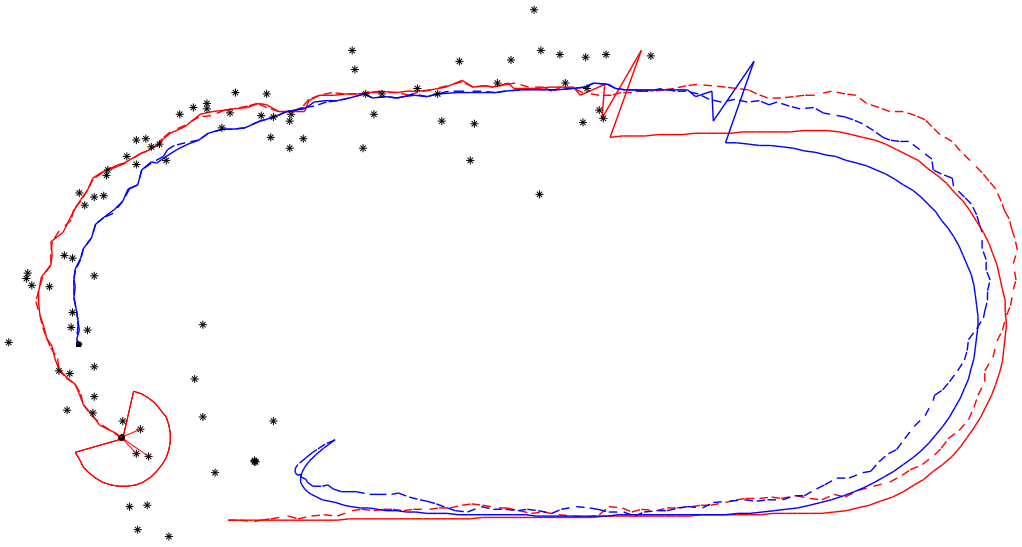

Figure 6: Lunar outpost simulation. The leader rover (illustrated in red) is capable of measuring landmarks (cross hairs), which may be beacons laid out by astronauts (structured environment), distinct features extracted from the terrain (unstructured environment), or both. The follower rover (illustrated in blue) can communicate, but is not equipped with the hardware to collect measurements (hence not able to conduct SLAM). However, once measurements are available to the leader, the follower is able to localize itself based on the leader-follower model.

3.2 Benefits of communication

In considering the best case performance of SLAM with exchange of leader-follower information, we examine the special case of when the shared N-landmark vector of the leader and follower rovers is fully observable (measurements from all N landmarks) by both rovers and compare the results to single-robot SLAM without communications; for both cases, we assume the landmark correspondences are known. Performances are shown for an increasing number of landmarks.

The intuition of Figure 7 is that multi-rover SLAM is most useful in terms of localization when the number of landmark observations between the two platforms is relatively low (i.e., localization improves due to the coupling of the rover states), yet landmark estimation, or mapping, may not significantly benefit in this case (Figure 8). Conversely, when the number of landmark observations is relatively high, the performance of multi-rover SLAM and single-rover SLAM may be equivalent in terms of localization, but multi-rover SLAM outperforms single-robot SLAM in terms of mapping.

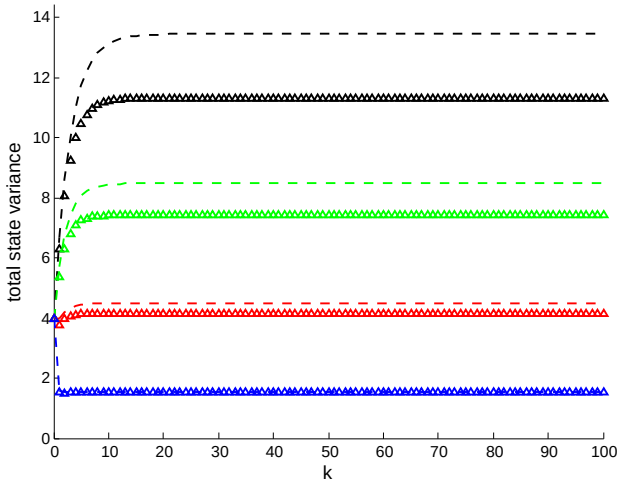

Figure 7: Rover state estimation variances for a fully observable N-landmark vector with $N \in \{1, 2, 5, 20\}$.

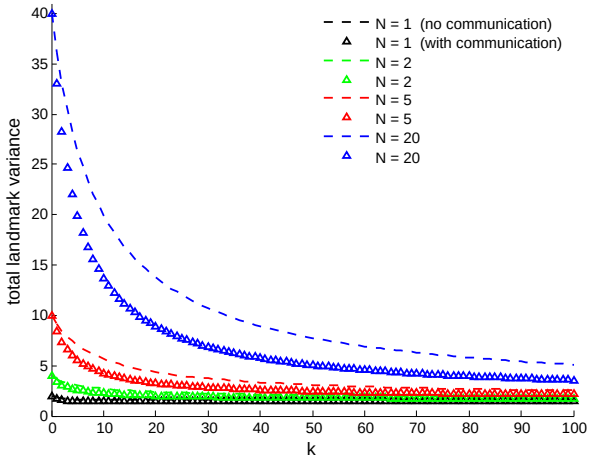

Figure 8: Landmark estimation variances for a fully observable N-landmark vector with $N \in \{1, 2, 5, 20\}$. The legend in this figure also applies to Figure 7.

Another benefit of communication can be seen from the lunar outpost simulation, which contains a "blind follower," meaning the follower rover is not capable of making landmark observations. Although the follower is incapable of conducting SLAM, it may still have localization capabilities within the formation under the leader-follower model (in spite of lacking the ability to measure landmarks); this ability may be useful in the case where a rover has a failure in sensor hardware.

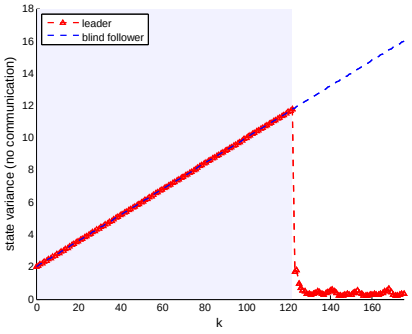

(a)

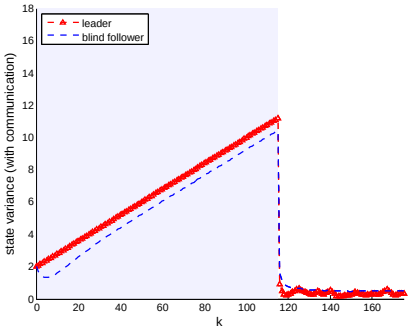

(b)

Figure 9: Lunar outpost simulation results showing (a) the increasing variance (uncertainty) of the blind follower state estimate without the use of communication and (b) the decrease in state estimation uncertainty of the blind follower when leader-follower information is communicated between the rovers. The shaded region shows when landmark measurements are not available to the leader rover.

4 Conclusions and future work

In this paper, we presented a leader-follower formation model for multi-rover SLAM as a means of information exchange. The kinematic and measurement models of the formation models are based on the equivalent models for single-robot SLAM using Kalman filters. The formation estimation model was applied to a space based application. The main results of this paper illustrate that multi-robot SLAM is useful for 1) localization when the number of landmark observations is relatively low and 2) for mapping when the number of landmark observations is relatively high. Future work includes developing a nonlinear SLAM formation model involving an arbitrary number of robots.

Acknowledgment

Sincere thanks are extended to the National Aeronautics and Space Administration for partially funding this work through the Harriett G. Jenkins Pre-doctoral Fellowship Program (JPFP).

References

[1] B. Dabrowski and M. Banaszkiewecz, "Multi-rover navigation on the lunar surface," *Advances in Space Research*, Vol 42, Issue 2, pp. 369–378, July 2008.

[2] B. Anderson and J. Moore, *Optimal filtering*, Prentice Hall, 1979.

[3] S. Thrun, D. Fox and W. Burgard, *Probabilistic robotics*, MIT Press, 2005.

[4] E. Nettleton, S. Thrun, H.F. Durrant-Whyte and S. Sukkarieh, "Decentralized SLAM with low-bandwidth communication for teams of vehicles," *Proc. of International Conference on Field and Service Robotics*, pp. 179-188, July 2003.

[5] L.L. Ong, Ridley M., Kim J., Nettleton E. and Sukkarieh S., "Six DoF decentralised SLAM," *Australian Conference on Robotics and Automation*, Brisbane, Australia, December 2003.

[6] S. Thrun and Y. Liu, "Multi-robot SLAM with sparse extended information filers," *Proceedings of the 11th International Symposium of Robotics Research (ISRR)*, 2005.

[7] D. Fox, J. Ko, K. Konolige, B. Limketkai, D. Schulz and B. Stewart, "Distributed multirobot exploration and mapping," *Proceedings of the IEEE*, Vol 94, No. 7, pp. 1325–1339, July 2006.

[8] R. Smith and P. Cheeseman, "On the representation and estimation of spatial uncertainty," *International Journal of Robotics Research*, Vol. 5, No.4, pp. 56-68, 1986.

[9] T. Balch and R. C. Arkin, "Behavior-based formation control for multirobot teams," *IEEE Trans. Robot. Automat.*, Vol. 14, No. 6, pp. 926–939, 1998.

[10] J. Fax and R. Murray, "Information flow and cooperative control of vehicle formations," *IEEE Trans. Auto. Control*, Vol. 49, No. 9, September 2004.

[11] G. Dissanayake, P. Newman, H.F. Durrant-Whyte, S. Clark, and M. Csobra, "A solution to the simultaneous localisation and mapping (SLAM) problem," *IEEE Trans. Robot. Automat.*, Vol. 17, No. 3, pp. 229–241, 2001.

[12] P. Gupta and P. R. Kumar, "The capacity of wireless networks," *IEEE Trans. Info. Theory*, Vol. 46, pp. 388-404, March 2000.